

Cyber Mobility Mirror for Enabling Cooperative Driving Automation: A Co-Simulation Platform

Zhengwei Bai¹, *Student Member, IEEE*, Guoyuan Wu², *Senior Member, IEEE*, Xuewei Qi, Kentaro Oguchi, Matthew Barth³, *Fellow, IEEE*

Abstract—Endowed with automation and connectivity, Connected and Automated Vehicles (CAVs) are meant to be a revolutionary promoter for Cooperative Driving Automation (CDA). Nevertheless, CAVs need high-fidelity perception information on their surroundings, which is available but costly to collect from various on-board sensors, such as radar, camera, and LiDAR, as well as vehicle-to-everything (V2X) communications. Therefore, precisely simulating the sensing process with high-fidelity sensor inputs and timely retrieving the perception information via a cost-effective platform are of increasing significance for enabling CDA-related research, e.g., development of decision-making or control module. Most state-of-the-art traffic simulation studies for CAVs rely on the situation-awareness information by directly calling on intrinsic attributes of the objects, which impedes the reliability and fidelity for testing and validation of CDA algorithms. In this study, a co-simulation platform is developed, which can simulate both the real world with a high-fidelity sensor perception system and the cyber world (or “mirror” world) with a real-time 3D reconstruction system. Specifically, the real-world simulator is mainly in charge of simulating the road-users (such as vehicles, bicyclists, and pedestrians), infrastructure (e.g., traffic signals and roadside sensors) as well as the object detection process. The mirror-world simulator is responsible for reconstructing 3D objects and their trajectories from the perceived information (provided by those roadside sensors in the real-world simulator) to support the development and evaluation of CDA algorithms. To illustrate the efficacy of this co-simulation platform, a roadside LiDAR-based real-time vehicle detection and 3D reconstruction system is prototyped as a study case.

Index Terms—Co-Simulation Platform; Connected and Automated Vehicles; Cooperative Driving Automation; 3D Object Detection and Reconstruction.

I. INTRODUCTION

WITH rapid development of the economy and society, the field of transportation is facing several major challenges caused by drastically increased traffic demands, such as improving traffic safety, mitigating traffic congestion, and reducing mobile source emissions. Cooperative Driving Automation (CDA) enabled by Connected and Automated Vehicles (CAVs) is regarded as a promising solution to the aforementioned challenges [1]. In the past few decades, several projects have been conducted to explore the potential of CDA. For instance, California PATH program [2] demonstrated the

improvement of traffic throughput by an automated platoon utilizing connectivity, and the European DRIVE C2X project [3] assessed cooperative system by large-scale field operational tests of various connected vehicle applications. These projects have demonstrated CDA to be a transformative path towards the next-generation transportation system, which is enabled by ubiquitous perception, seamless communication, and advanced artificial intelligence technologies.

Given the fact that the cost of large-scale real-world deployment is prohibitive, it is imperative to design and assess CDA systems based on simulation. For instance, as one key component of a CDA system, connected and automated vehicle (CAV) technologies heavily rely on simulation to comprehensively assess their performance in terms of safety, efficiency, and environmental sustainability. Therefore, simulation platforms for CDA are of great significance and their development receives much attention.

Additionally, to enable CDA, accurate perception information can lay a solid foundation, which requires inputs from different types of high-fidelity sensors, such as radar, camera, and LiDAR. Direct implementation of these sensors to perceive the real-world environment may be costly or time consuming, and in some cases, restricted by application scenarios. Thus, simulation platforms with high-fidelity sensor modeling and perception capability would provide a cost-effective alternative solution to CDA-related research.

Up to date, many existing traffic simulators have been developed to test various aspects of CDA. For instance, CARLA [4] and SVL [5] are designed for modeling autonomous vehicles (AVs), while SUMO [6] targets microscopic traffic flows. From the perspective of sensing fidelity, most existing studies directly use intrinsic attributes of target objects, without considering potential imperfection of perception for CDA models. This considerably limits the transferability and reliability for real-world deployment of these CDA models. To the best of our knowledge, this paper is the first attempt to integrate the entire deep learning-based perception pipeline into simulator to create a cyber mobility mirror (CMM) system, in which simulated traffic objects are authentically perceived and reconstructed with 3D representation. The high-level CDA model can leverage such perceived information from the module output in a CMM system rather than intrinsic attributes of target objects, to improve model fidelity and validate the system with more confidence.

The systematic structure of CMM based on a co-simulation platform is shown in Figure 1, where one simulator is designed

Zhengwei Bai and Matthew Barth are with the Department of Electrical and Computer Engineering, University of California at Riverside, Riverside, CA 92507 USA (e-mail: zbai012@ucr.edu).

Guoyuan Wu is with the Center for Environmental Research and Technology, University of California at Riverside, Riverside, CA 92507 USA.

Xuewei Qi and Kentaro Oguchi are with the Toyota North America R&D Labs, Mountain View, CA 94043, USA.

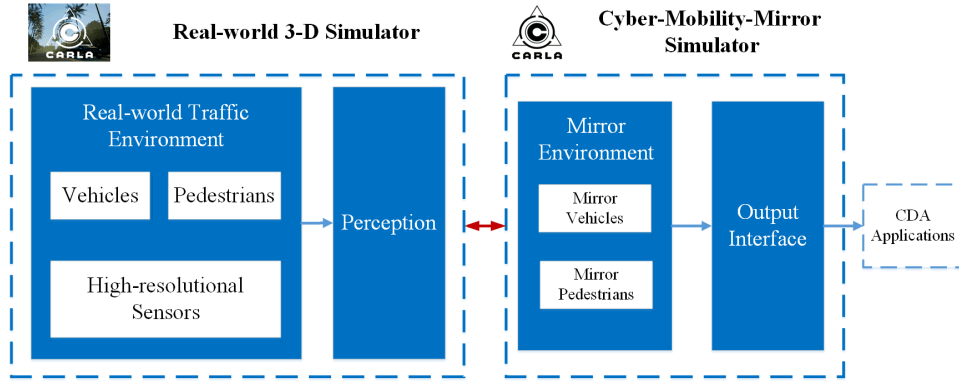


Fig. 1. The systematic architecture for the proposed co-simulation based CMM.

to model the real-world traffic environment and the authentic perception pipeline, while the other simulator is used to work as a mobility mirror, i.e., reconstructing the perceived objects and presenting them. The output interface provides readily retrieved post-perception data for CDA applications.

The main contributions in this paper can be summarized as follows: (1) we propose a cyber mobility mirror (CMM) architecture for enabling CDA; (2) we design and develop a prototype CMM system using a CARLA-based co-simulation platform; and (3) we conduct a case study of roadside LiDAR based vehicle detection and reconstruction to showcase the functionality and feasibility of the proposed co-simulation platform.

The rest of this paper is organized as follows. A brief background about traffic simulation and object perception is given in Section 2. In Section 3, we first introduce the concept of CMM and then describe the design and development of the prototype system based on co-simulation. In Section 4, we present a case study for detecting and reconstructing vehicles based on roadside LiDAR sensing and deep learning methods, followed by the conclusion and discussion in Section 5.

II. BACKGROUND

Simulation plays a crucial role for enabling cooperative driving automation, such as assessment of CAV cooperative perception algorithms and decision making/control models. High-fidelity simulated sensor information lays a solid foundation for these high-level CDA algorithms and models. In this section, we briefly review the background information for simulators enabling CDA and object detection.

A. Simulators Enabling Cooperative Driving Automation

1) *Microscopic Traffic Simulators*: To model the evolution of traffic states based on traffic dynamics and interactions between traffic objects, microscopic traffic simulators have been developed for decades and greatly stimulating the development of intelligent transportation systems [7]. These simulators mainly consist of three components: (1) transportation network defining road topology; (2) traffic generator creating traffic flows with certain demand distributions; and (3) microscopic

traffic flow control strategies, including traffic signal management, vehicle driving behaviors and moving strategies for pedestrians.

Several simulation platforms are of great popularity in CDA research, such as VISSIM [8], Aimsun [9], and SUMO (Simulation of Urban MObility) [10]. Specifically, VISSIM and Aimsun are widely used in dealing with multi-modal traffic flow simulation due to their capabilities of providing fundamental 3D preview and statistical simulation results. SUMO is an open-source, highly portable, microscopic and continuous traffic simulation package designed to handle large networks [6]. Additionally, high compatibility to connect and interact with different kinds of external simulators, e.g., OMNeT++ [11], CARLA, etc., is one of the key features of SUMO. These microscopic traffic simulators mainly focus on general assessment for traffic dynamic performance at the network level under different traffic scenarios. Nevertheless, the design and assessment of CDA-based cooperative perception, decision-making or control models highly rely on the fidelity of sensor data, which is a major challenge for these conventional simulators. In recent years, simulators that are capable of modeling high-fidelity sensors gain more and more interests, which are introduced in the following section.

2) *Autonomous Driving Simulators*: With the development of CDA, especially autonomous driving technologies (ADTs) [12], the requirement of high-fidelity sensors in simulators has gained more and more attention. In recent years, several autonomous driving simulators quipped with high-fidelity sensors have been developed based on game engines, such as Unity [13] and Unreal Engine [14]. For instance, AirSim [15], SVL, and CARLA, have the capability to offer physically and visually realistic simulations for autonomous vehicle technologies (AVTs) as well as CDA systems. Specifically, AirSim includes a physics engine that can operate at a high frequency for real-time hardware-in-the-loop (HIL) simulations with support for popular protocols, such as MavLink [16]. SVL is a high-fidelity simulator for AVTs, which provides end-to-end and full-stack simulation that is ready to be hooked up with several open-source autonomous driving stacks, such as Autoware [17] and Apollo [18]. CARLA, an open-source simulator for autonomous driving, supports flexible specification of sensor suites and environmental conditions. In addition to open-

source codes and protocols, CARLA provides open digital assets (e.g., urban layouts, buildings, and vehicles) that can be used in a friendly manner for researchers.

These simulators have been developed from the ground up to support development, training, and validation of AVTs, enabling the development of CDA. They have the capacity to assess the CDA system in a cost-effective manner as well as to provide high-fidelity sensing information.

Although having these existing simulators, researchers still get struggled by the imperative assumption that perception data (e.g., location, velocity, rotation, etc.) is collected directly from intrinsic attributes of simulation engines, when they develop and evaluate their high-level CAV functions, such as decision-making or control methods for CDA. Therefore, to develop a generic platform that can not only support physically and visually realistic simulation but also provide perception data based on high-fidelity sensor information, is still a research gap for enabling CDA system research and development.

B. Traffic Object Detection

Traffic object detection plays a crucial and fundamental role for enabling CDA, and it can be roughly divided into two major types: (1) conventional model-based algorithms, such as edge detection and segmentation; and (2) data-driven methods based on deep neural networks to extract hidden features from input signals and then to generate detected results. The following section will briefly introduce several state-of-the-art methods for each type.

1) *Model-based Methods*: At the early stage of traffic detection, sensors with low-computational power are widely used, such as loop detector, radar, ultrasonic, etc. Although most of them are still implemented in contemporary transportation systems, they suffer from different kinds of innate problems, such as detecting uncertainties, traffic disruption at installation, and high maintenance costs [19]. With the development of computer vision (CV) technology and improvement of computational power, camera-based traffic object detection has been widely developed. For instance, Aslani and Mahdavi-Nasab [20] tried to gather useful information from stationary cameras for detecting moving objects in digital videos based on optical flow estimation. In the situations where limited memory and computing resources are available, Lee et al. [21] presented a moving object detection method for real-time traffic surveillance applications based on a genetic algorithm.

Recently, LiDAR sensor is increasingly implemented for traffic object detection tasks due to its advantage of having higher tolerance of lighting conditions and accuracy of relative distance. Regarding traditional methods to deal with 3D point cloud, one popular workflow is: (1) background filtering; (2) traffic object clustering; and (3) object classification [22]. Additionally, LiDAR point cloud can also be used to identify lane markings [23], [24]. Although some traditional methods have been applied to 3D point cloud, greater potential of LiDAR data should be tapped by data-driven methods (e.g., deep learning) which are introduced next.

2) *Data-driven Methods*: The development of deep neural networks (DNNs) has significantly improved the possibility

for dealing with large-scale data, such as high-fidelity images or 3D point cloud. With the great success of deep learning in image recognition area [25], [26], many DNN-based models have been implemented in object detection for traffic scenarios using cameras or LiDAR sensors.

Chabot et al. [27] presented an approach called *Deep MANTA*, for multi-task vehicle analysis based on monocular image. In terms of different lighting conditions, Che-Tsung Lin developed a nighttime vehicle detection method based on image style transfer [28]. Chen et al. [29] proposed a shallow model named *Concatenated Feature Pyramid Network* (CFPN) to detect smaller objects in traffic flow from fish-eye camera images.

Additionally, 3D-LiDAR also gets more popular in traffic object detection. For instance, Asvadi et al. [30] presented an algorithm named *DepthCN* which used deep convolutional neural networks (CNNs) for vehicle detection. Considering the real-time requirement for autonomous driving applications, Zeng et al. [31] proposed a real-time 3D vehicle detection method by utilizing pre-ROI-pooling convolution and pose-sensitive feature map. Simon et al. [32] proposed an Euler-Region-Proposal for real-time 3D object detection with point clouds, called *ComplexYolo*, which is capable of generating rotated bounding boxes for 3D objects. For CDA applications, traffic object detection needs meticulous consideration. Thus, in our CMM co-simulation framework, ComplexYolo model is adapted with customized improvements for real-time vehicle and pedestrian detection.

III. PLATFORM STRUCTURE AND DESIGN

This section will describe the concept of cyber mobility mirror (CMM) in detail and the system architecture of the co-simulation platform based on CARLA. Specifically, the design and development of real-world simulator, mirror simulator, data communication module and LiDAR-based perception module will be introduced.

A. CMM Based Co-Simulation Architecture

As aforementioned, the cyber mobility mirror can further tap potential of the traffic object surveillance systems to enable cooperative driving automation (CDA), especially for routing planning, cooperative decision-making and motion control. From this perspective, this paper presents a co-simulation platform based on the CMM concept. Figure 2 demonstrates the concept of CMM with an intersection scenario and the system architecture of the CMM-based co-simulation.

In Figure 2, the upper left part represents the real-world traffic scenario at an intersection, equipped with several roadside high-fidelity sensors, e.g., camera and 3D-LiDAR, roadside computing server and communication system. High-fidelity sensor data is retrieved by the roadside server, in which perception tasks are executed, e.g., traffic object detection, classification, tracking, and motion prediction. Then perception results are encoded and transmitted to the CMM server via communication networks, e.g., cellular, DSRC or WLAN. The upper right part of Figure 2 represents the mirror environment, which reconstructs 3D objects based on perception information

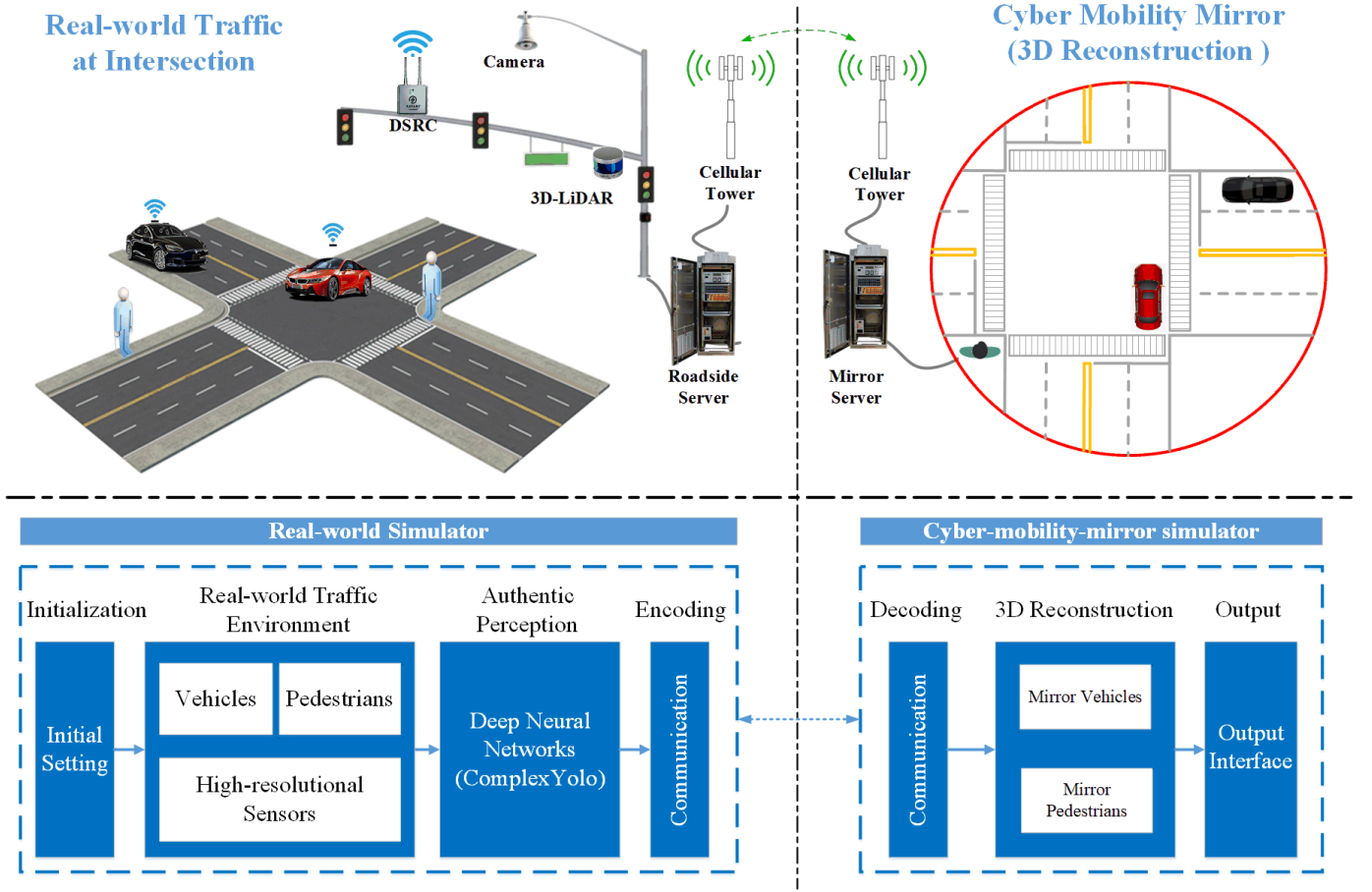


Fig. 2. The visualization for CMM concept in real-world intersections (upper part) and CMM-based co-simulation architecture (lower part).

and outputs to CDA applications, e.g., collision avoidance, smart lane selection [33], and cooperative eco-driving [34].

As aforementioned, building a comprehensive traffic object perception system in the real world requires plenty of hardware and labor resources. In this paper, we propose a cost-effective means to emulate the real-world traffic environment via a game-engine based simulator, CARLA, which has the capability of generating traffic environment and high-fidelity sensor information. The structure of the real-world simulator, demonstrated in the lower left part of Figure 2, consists of four modules: (1) initialization of system settings; (2) configuration of CARLA-based traffic environment with traffic objects and equipped sensors; (3) authentic perception using DNNs, such as ComplexYolo model; and (4) data encoding for communication. As shown in the lower right part of the figure, the Mirror Simulator is also developed based on CARLA and consists of three components: (1) decoding of the communicated data; (2) 3D reconstruction for vehicles and pedestrians; and (3) output interface for CDA applications to readily retrieve the post-perception data.

In this paper, we present the basic concept of CMM and design the concrete workflow of a roadside-sensor-based intersection surveillance scenario. In the following section of co-simulation design and development, we focus on: (1) applying roadside 3D-LiDAR for perception; (2) object detection and

classification for vehicles and pedestrians; and (3) multi-vehicle 3D reconstruction for enabling CDA applications.

B. Real-world Simulator Design

The main purpose of the real-world simulator is to generate a virtual environment based on CARLA to emulate the real-world traffic environment. Main sub-tasks of the development effort are shown as follows.

1) *Traffic scenario design*: CARLA has provided several well-developed virtual towns with different road maps and textures. In this paper, we implement “town03” as our fundamental traffic map and select a target intersection for research. This is shown in the left part of Figure 3. Additionally, we can generate vehicles and pedestrians via CARLA-based python scripts. The right part of Figure 3 shows a specific top-down view of the traffic scenario with vehicles, pedestrians, and a 3D-LiDAR installed at the target intersection. The traffic is generated via CARLA interface with respect to certain traffic demand and the traffic signals are controlled by the built-in traffic signal manager in CARLA.

2) *Infrastructure based sensor design*: In this paper, we implement a roadside 3D-LiDAR as our main sensor. The roadside LiDAR is installed at the southwest corner of the target intersection, which is demonstrated in Figure 3 (the LiDAR is installed below the arm of the traffic signal pole).

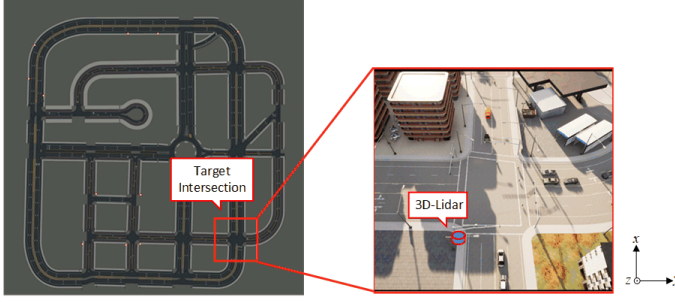


Fig. 3. Traffic scenario design and 3D-LiDAR location.

Specifically, detailed settings about the roadside 3D-LiDAR are described later in Table 1. To reduce the concern on transferability of the deployed deep neural network model, we resemble the LiDAR setups as used to obtain the KITTI dataset [35]. This means that the pitch, yaw and roll of the LiDAR are set as zeros in CARLA global coordinate, as shown in the right part of Figure 3. Specifically, the LiDAR intensity is calculated by the following equation:

$$I = I_0 \cdot e^{-a \cdot d} \quad (1)$$

where I_0 represents the initial intensity value (equals to 1 in this study); a represents attenuation coefficient, depending on the sensor's wavelength and atmospheric conditions (which can be modified by the LiDAR attribute "atmosphere_attenuation_rate"); and d is the distance from the hit point to the sensor. More details about the implemented 3D-LiDAR are described in the case study section.

3) *Deep Learning Based Perception Methods*: In this paper, we apply the ComplexYolo model [32] as our fundamental 3D object detection method. The basic pipeline of ComplexYolo model is demonstrated by Figure 4.

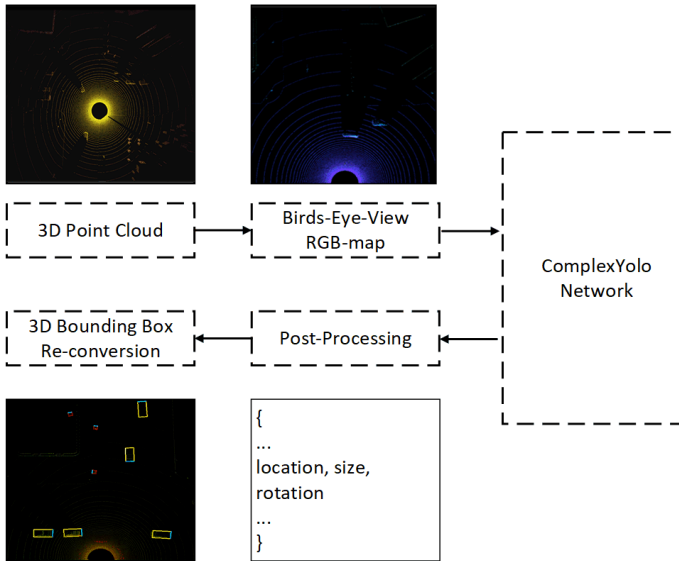


Fig. 4. ComplexYolo based real-time multi-class traffic object detection.

In ComplexYolo model, raw 3D-LiDAR data is firstly cut into a certain shape with respect to the target region; then the 3D point cloud is processed into bird's-eye-view RGB

map based on different features; the CNN-based ComplexYolo network generates detection outputs based on the RGB map; moreover, post-processing is implemented to filter detection results with respect to certain thresholds; finally, 3D bounding boxes are calculated and displayed on the RGB map image. The optimization loss function L for ComplexYolo is defined as:

$$L = L_{Yolo} + L_{Euler} \quad (2)$$

where L_{Yolo} is defined as the sum of squared errors using the multi-part loss introduced in YOLO [36] and YOLOv2 [37], while the Euler regression part L_{Euler} is defined to handle complex numbers, which has a closed mathematical space for angle comparisons [32]. The implementation details of the ComplexYolo model in this paper will be introduced in the case study section.

C. Mirror Simulator Design

The main purposes of the Mirror Simulator are: (1) performing 3D reconstruction for the perceived objects; and (2) providing readily used output interface for CDA applications.

In this paper, the Mirror Simulator is also developed based on CARLA simulator. The same CARLA town, "town03", is used to build this mobility mirror, as shown on the left in Figure 3. The 3D reconstruction procedure consists of two parts: (1) decoding post-perception data received from the real-world simulator via communication; and (2) generating 3D traffic objects with respect to the decoding data based on CARLA Python APIs (Application Programming Interfaces). Specifically, the message decoding method is further described in next section.

D. Information Synchronization and Communication Protocol

1) *Information Synchronization*: For this co-simulation platform, we design the information synchronization approach based on the server-client architecture in CARLA [4]. The sequence diagram for information synchronization among components is demonstrated in Figure 5.

In CARLA platform, the server runs the simulation (i.e., updates the information), while the client retrieves information. Specifically, as shown in Figure 5, the Traffic Generator (CARLA Client 1-1) is responsible for simulation initialization or stopping request; the Real-world Simulator (CARLA Server 1) runs the simulation for real-world traffic and the LiDAR sensor; the Detection Generator (CARLA Client 1-2) is designed to generate 3D object detection results by utilizing the ComplexYolo model. The detection results are encoded into post-perception data and transmitted to the Mirror Simulator (CARLA Server 2) via TCP/IP communications. Finally, the Mirror Output (CARLA Client 2-1) can retrieve the mirrored objects' information, e.g., vehicle center location, bounding box dimension and orientation, from the Mirror Simulator.

2) *Communication Protocol*: In this paper, TCP/IP [38] protocol is implemented to transmit post-perception data from the Real-world Simulator to the Mirror Simulator. Specifically, before transmitting, object detection results are encoded based on JSON protocol [39], which include locations and orientations of the objects. For data encoding at the Mirror Simulator,

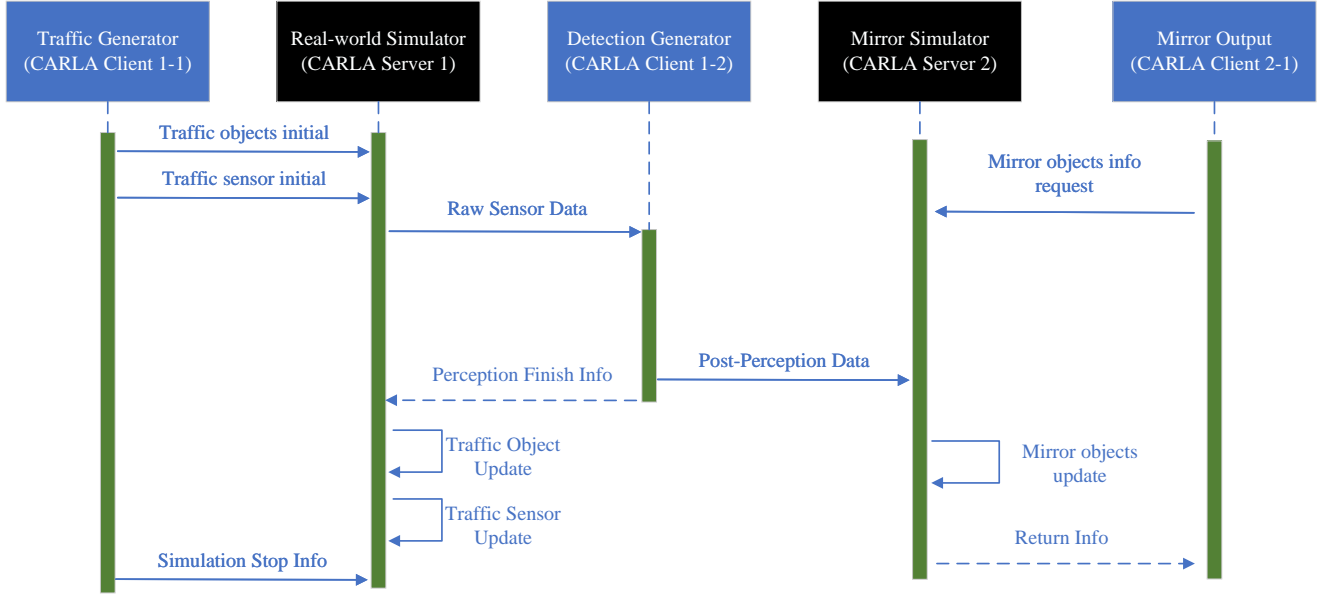


Fig. 5. Sequence diagram for information synchronization among components.

the JSON data is decomposed according to the data structure in CARLA.

IV. CASE STUDY: REAL-TIME VEHICLE DETECTION AND 3D RECONSTRUCTION

A. System Setup

Both the Real-world Simulator and Mirror Simulator run under the synchronous mode of CARLA, which means the server can update the simulator information at the same time step with clients. In this paper, the simulation frequency is set as 10 Hz. The network traffic demand is set to be 100 vehicles (driving around the town according to the default routing strategy and autopilot method in CARLA) [4].

For the 3D-LiDAR implemented in this paper, attributes of the LiDAR sensor are shown in Table I.

B. CARLA-based 3D-LiDAR Dataset

To implement the ComplexYolo model in our co-simulation platform, a well-defined 3D-LiDAR dataset with ground-truth label is required. Although CARLA provides a comprehensive

Python API for data retrieving and object controlling, a built-in dataset generator is still missing. Therefore, based on the existing CARLA Python API and the KITTI dataset structure, we develop a CARLA-based 3D-LiDAR Dataset. Visualization of the 3D point cloud and rotated 3D ground-truth bounding boxes of one frame data in our CARLA-based Dataset is shown in Figure 6. The code for generating LiDAR-based training dataset is available at: https://github.com/zwbai/CARLA_Dataset_Generate.

C. Vehicle Detection

1) *Point Cloud Preprocessing*: In this paper, our target range for the vehicle detection is defined as a 50 meters by 50 meters area Ω with respect to the location of LiDAR, which is demonstrated as the gray square box in Figure 6. To reduce the impact from 3D LiDAR points out of the target range, the raw point cloud data $P = \{[x, y, z, i]^T \mid [x, y, z]^T \in \mathbb{R}^3, i \in [0, 1]\}$ is geo-fenced with a size of 50 meters by 50 meters. Specifically, the 3D point set within the target area P_Ω is defined as: $P_\Omega = \{[x, y, z, i]^T \mid x \in [0, 50m], y \in [-25m, 25m], z \in$

TABLE I
PARAMETER CONFIGURATION AND DESCRIPTION FOR 3D-LiDAR

Parameters	Default	Description
channels	64	Number of lasers
height	1.73m	Height with respect to the road surface
range	100.0m	Maximum distance to measure/ray-cast in meters
points_per_second	500000	Points generated by all lasers per second
rotation_frequency	10.0 Hz	LiDAR rotation frequency
upper_fov	2.0	Angle in degrees of the highest laser
lower_fov	-24.9	Angle in degrees of the lowest laser
atmosphere_attenuation_rate	0.05	Coefficient that measures the LiDAR intensity loss
noise_stddev	0.0002	Standard deviation of the noise model to disturb each point along the vector of its ray-cast

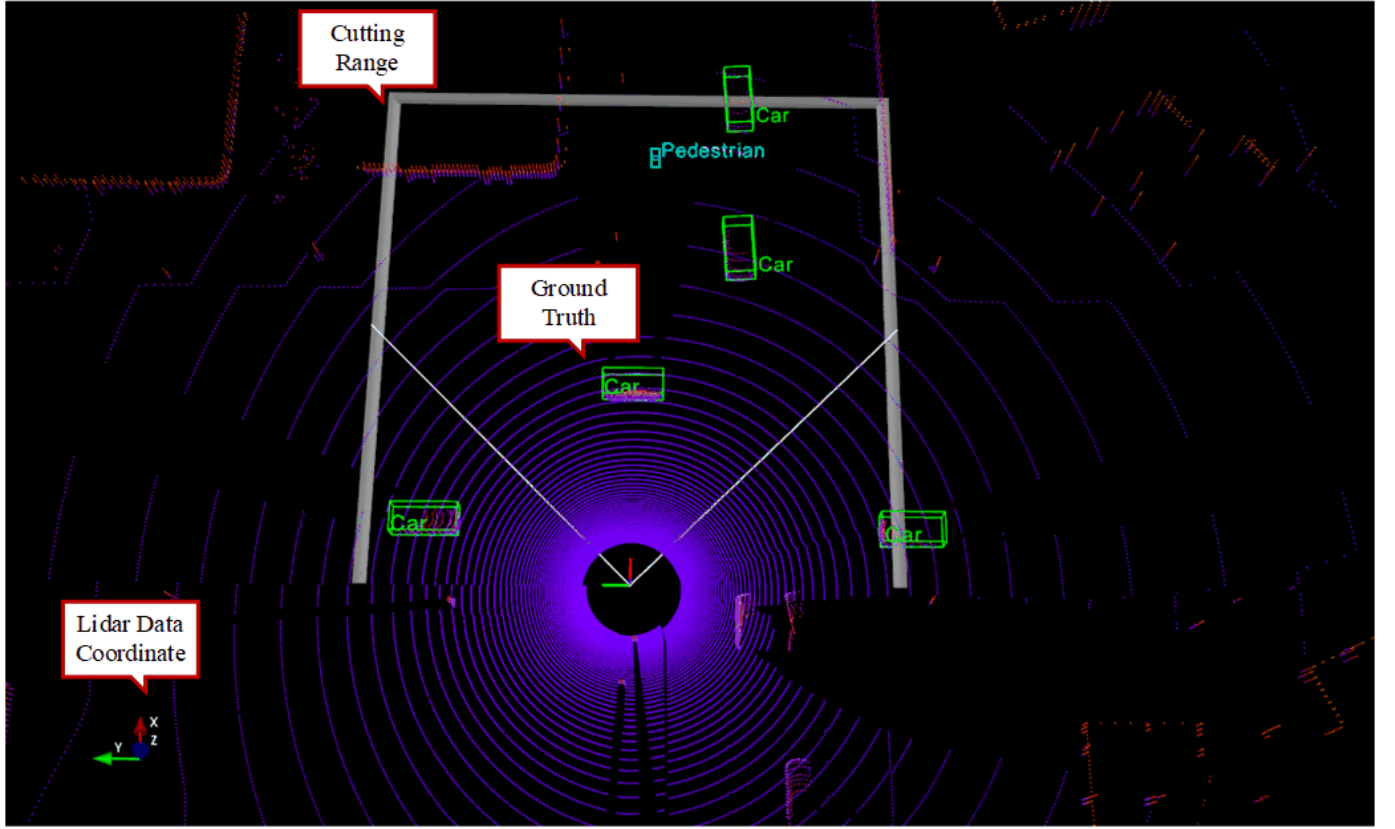


Fig. 6. Visualization of the CARLA-based Dataset: 3D point cloud and ground truth label.

$[-2m, 1.25m], i \in [0, 1]$. Additionally, ground truth labels are collected according to the objects within the target range.

2) *BEV Image Construction*: The 3D points within the target range are then normalized by the following equations:

$$\begin{bmatrix} \tilde{x} \\ \tilde{y} \\ \tilde{z} \end{bmatrix} = \begin{bmatrix} \frac{h}{range_x} & 0 & 0 \\ 0 & \frac{h}{range_y} & 0 \\ 0 & 0 & 1 \end{bmatrix} \begin{bmatrix} x \\ y \\ z \end{bmatrix} + \begin{bmatrix} 0 \\ 0.5w \\ 0 \end{bmatrix} \quad (3)$$

where $range_x$ and $range_y$ represent the range along x-axis direction and y-axis direction, respectively; w and h denote the weight and height of the BEV image, respectively. Specifically, $[xyz]^T$ and $[\tilde{x} \tilde{y} \tilde{z}]^T$ represent the input 3D-LiDAR point and the normalized 3D-LiDAR point, respectively.

Then the three-feature maps, i.e., R-map, G-map, and B-map can be defined according to the density, height, and intensity information, respectively, as shown in the following [32].

$$\begin{aligned} z_r(S_j) &= \min(1.0, \log(N + 1)/64, N = |P_{\Omega \rightarrow j}|) \\ z_g(S_j) &= \max(P_{\Omega \rightarrow j} \cdot [0, 0, 1]^T) \\ z_b(S_j) &= \max(I(P_{\Omega \rightarrow j})) \end{aligned} \quad (4)$$

where S_j represents a specific grid cell of RGB-map; z_r , z_g and z_b represent three channels for RGB-map; I represents the intensity of LiDAR point and N describes the number of points mapped from $P_{\Omega \rightarrow i}$ to S_j .

3) *Data Training*: Based on the CARLA dataset, we train the ComplexYolo model from scratch via stochastic gradient descent with a weight decay of 0.0005 and momentum of 0.9.

For the dataset preparation, we subdivide the training set with 80% for training and 20% for validation. The learning rate is set as 0.001 for initialization and gradually decreased along 1000 training epochs. For regularization, we implement batch normalization. For activation functions, leaky rectified linear activation function, defined as follows, is used except the last layer of the convolution neural network (CNN) where a linear activation function $f(x) = x$ is used.

$$f(x) = \begin{cases} x, & x > 0 \\ 0.1x, & otherwise \end{cases} \quad (5)$$

D. Results and Analysis

1) *Training Results*: Figure 7, Figure 8 and Figure 9 demonstrate the overall performance of the training results. Specifically, Figure 7 shows the training loss for the location and the volume of the objects. Figure 8 displays the training loss for the yaw angle of the objects and Figure 9 demonstrates the performance of recall@50, recall@75, precision, and detection confidence along the training process.

2) *Evaluation Results on Testing Dataset*: Figure 10 demonstrates the visualization of object detection results for the authentic perception model in the Real-world Simulator. Specifically, vehicles and pedestrians are bounded with yellow and red boxes, respectively. In addition, blue edges of the bounding boxes represent the forward direction of the detected objects.

Figure 10 validates the feasibility of our CMM-based co-simulation platform. Vehicles and pedestrians are detected via

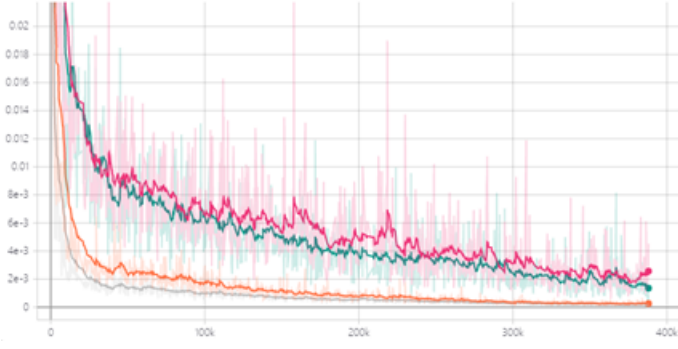


Fig. 7. Training loss for location x (pink curve), location y (green curve), weight of bounding box (gray curve) and height of bounding box (orange curve) respectively.

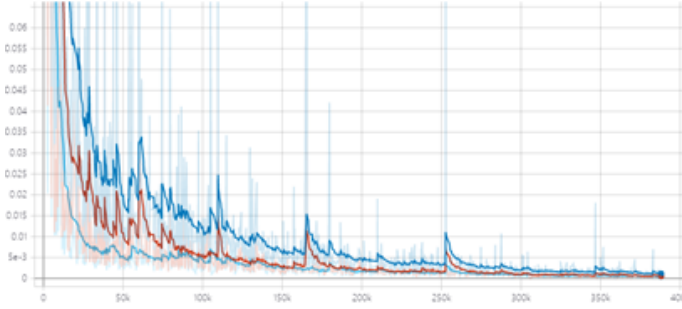


Fig. 8. Training loss for (dark-blue curve), imaging part of (dark-yellow curve) and real part of (light-blue curve) respectively.

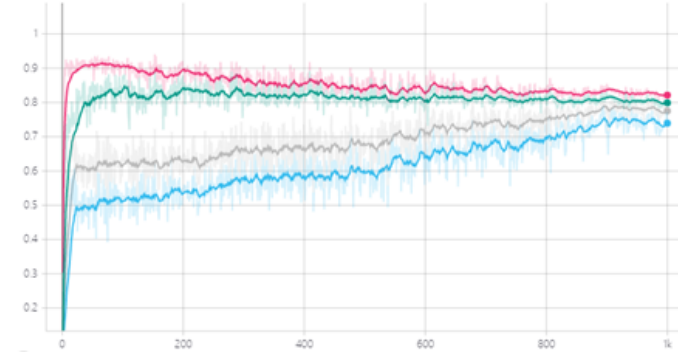


Fig. 9. Validation results along the training process, including recall (pink curve), AP (green curve), f1 (gray curve) and precision (light-blue curve) respectively.

the roadside-based LiDAR and the associated digital replica are reconstructed in the mobility mirror simulator. Due to the detection range and accuracy of the selected model (i.e., ComplexYolo), some objects will be missed. Nevertheless, our platform is generic and highly compatible with different detection models and the results can be improved with the advances in SOTA detection methods.

The evaluation results on testing dataset are demonstrated in Table II. It is evident that the detection results for vehicles are much better than pedestrians. A hypothesis is that fewer LiDAR points would be reflected from pedestrians than vehicles and pedestrians are more susceptible to occlusion, due to their smaller sizes.

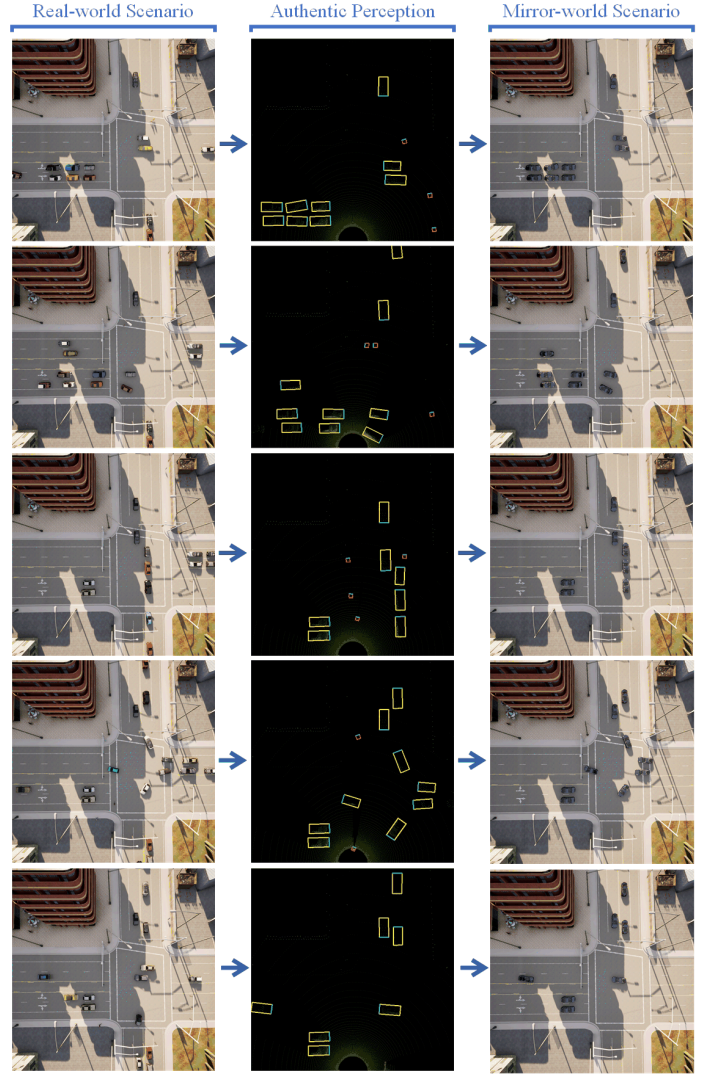


Fig. 10. Visualization of object detection results: (1) the left-column images represent the top-down views of the traffic at the intersection; (2) the middle-column images represent the detection results with rotated bounding boxes; and (3) the right-column images show 3D reconstruction results in the Mirror Simulator.

TABLE II
DETAILS ABOUT THE EVALUATION RESULTS (IN %)

Evaluation criteria		Precision	Recall	AP	F1
Object Class	Car	91.94	92.97	92.51	92.46
	Pedestrian	68.71	66.12	59.16	67.39

In general, Figure 10 shows the key pipeline of our CMM-based co-simulation platform, i.e., generating authentic detection results based on high-fidelity sensors and 3D reconstructing the traffic objects for external CDA applications, which demonstrates functionality and feasibility of the co-simulation platform.

V. CONCLUSION AND DISCUSSION

To enable cooperative driving automation (CDA), simulators are imperative to comprehensively support the design and assessment of various applications. Moreover, authen-

tic perception based on high-resolution sensors is of great significance for CDA development. To the best of authors' knowledge, this paper is the first attempt to design and develop a co-simulation platform to prove the cyber mobility mirror (CMM) concept, which can both emulate high-resolution sensors and provide readily retrieved perception information. Specifically, the co-simulation platform consists of two main sub-simulators: (1) the Real-world Simulator for emulating the real-world traffic environment and (roadside) sensors and generating the authentic perception data; and (2) the Mirror Simulator for 3D reconstructing traffic objects and providing a readily retrieved interface for downstream CDA applications to access the location and orientation information of target traffic objects. A case study is conducted for real-time vehicle detection and 3D reconstruction in an intersection scenario, which demonstrates the performance of the vehicle detection model as well as the functionality and feasibility of the co-simulation platform.

In this paper, we develop a preliminary framework for CMM and validate it with simulation. A natural future step would be to realize the system in the real world, but there are some open issues deserving further exploration. For instance, we need to overcome disparities in the features between sensor data from simulator and that in reality. We need to investigate the model transferability issue, i.e., to design a model that can be trained on simulation and implemented in the real-world scenarios without necessities or much effort in re-training the model or fine tuning parameters.

ACKNOWLEDGMENTS

This research was funded by the Toyota Motor North America InfoTech Labs. The contents of this paper reflect the views of the authors, who are responsible for the facts and the accuracy of the data presented herein. The contents do not necessarily reflect the official views of the Toyota Motor North America.

REFERENCES

- [1] D. J. Fagnant and K. Kockelman, "Preparing a nation for autonomous vehicles: opportunities, barriers and policy recommendations," *Transportation Research Part A: Policy and Practice*, vol. 77, pp. 167–181, 2015.
- [2] J. A. Misener and S. E. Shladover, "Path investigations in vehicle-roadside cooperation and safety: A foundation for safety and vehicle-infrastructure integration research," in *2006 IEEE Intelligent Transportation Systems Conference*. IEEE, 2006, pp. 9–16.
- [3] R. Stahlmann, A. Festag, A. Tomatis, I. Radusch, and F. Fischer, "Starting european field tests for car-2-x communication: the drive c2x framework," in *18th ITS World Congress and Exhibition*, 2011, p. 12.
- [4] A. Dosovitskiy, G. Ros, F. Codevilla, A. Lopez, and V. Koltun, "Carla: An open urban driving simulator," in *Conference on robot learning*. PMLR, 2017, pp. 1–16.
- [5] G. Rong, B. H. Shin, H. Tabatabaee, Q. Lu, S. Lemke, M. Možeiko, E. Boise, G. Uhm, M. Gerow, S. Mehta *et al.*, "Lgsvl simulator: A high fidelity simulator for autonomous driving," in *2020 IEEE 23rd International Conference on Intelligent Transportation Systems (ITSC)*. IEEE, 2020, pp. 1–6.
- [6] P. A. Lopez, M. Behrisch, L. Bieker-Walz, J. Erdmann, Y.-P. Flötteröd, R. Hilbrich, L. Lücken, J. Rummel, P. Wagner, and E. Wießner, "Microscopic traffic simulation using sumo," in *2018 21st International Conference on Intelligent Transportation Systems (ITSC)*. IEEE, 2018, pp. 2575–2582.
- [7] J. Barceló *et al.*, *Fundamentals of traffic simulation*. Springer, 2010, vol. 145.
- [8] M. Fellendorf and P. Vortisch, "Microscopic traffic flow simulator vissim," in *Fundamentals of traffic simulation*. Springer, 2010, pp. 63–93.
- [9] J. Barceló and J. Casas, "Dynamic network simulation with aimsun," in *Simulation approaches in transportation analysis*. Springer, 2005, pp. 57–98.
- [10] M. Behrisch, L. Bieker, J. Erdmann, and D. Krajzewicz, "Sumo—simulation of urban mobility: an overview," in *Proceedings of SIMUL 2011, The Third International Conference on Advances in System Simulation*. ThinkMind, 2011.
- [11] A. Varga, "Omnet++," in *Modeling and tools for network simulation*. Springer, 2010, pp. 35–59.
- [12] B. R. Kiran, I. Sobh, V. Talpaert, P. Mannion, A. A. Al Sallab, S. Yogamani, and P. Pérez, "Deep reinforcement learning for autonomous driving: A survey," *IEEE Transactions on Intelligent Transportation Systems*, 2021.
- [13] A. Juliani, V.-P. Berges, E. Teng, A. Cohen, J. Harper, C. Elion, C. Goy, Y. Gao, H. Henry, M. Mattar *et al.*, "Unity: A general platform for intelligent agents," *arXiv preprint arXiv:1809.02627*, 2018.
- [14] B. Karis and E. Games, "Real shading in unreal engine 4," *Proc. Physically Based Shading Theory Practice*, vol. 4, no. 3, 2013.
- [15] S. Shah, D. Dey, C. Lovett, and A. Kapoor, "Airsim: High-fidelity visual and physical simulation for autonomous vehicles," in *Field and service robotics*. Springer, 2018, pp. 621–635.
- [16] A. Koubâa, A. Allouch, M. Alajlan, Y. Javed, A. Belghith, and M. Khalgui, "Micro air vehicle link (mavlink) in a nutshell: A survey," *IEEE Access*, vol. 7, pp. 87 658–87 680, 2019.
- [17] S. Kato, S. Tokunaga, Y. Maruyama, S. Maeda, M. Hirabayashi, Y. Kit-sukawa, A. Monrroy, T. Ando, Y. Fujii, and T. Azumi, "Autoware on board: Enabling autonomous vehicles with embedded systems," in *2018 ACM/IEEE 9th International Conference on Cyber-Physical Systems (ICCPs)*. IEEE, 2018, pp. 287–296.
- [18] F. Graf, *Apollo*. Routledge, 2008.
- [19] J. Guerrero-Ibáñez, S. Zeadally, and J. Contreras-Castillo, "Sensor technologies for intelligent transportation systems," *Sensors*, vol. 18, no. 4, p. 1212, 2018.
- [20] S. Aslani and H. Mahdavi-Nasab, "Optical flow based moving object detection and tracking for traffic surveillance," *International Journal of Electrical, Computer, Energetic, Electronic and Communication Engineering*, vol. 7, no. 9, pp. 1252–1256, 2013.
- [21] G. Lee, R. Mallipeddi, G.-J. Jang, and M. Lee, "A genetic algorithm-based moving object detection for real-time traffic surveillance," *IEEE signal processing letters*, vol. 22, no. 10, pp. 1619–1622, 2015.
- [22] J. Wu, H. Xu, J. Zheng, and J. Zhao, "Automatic vehicle detection with roadside lidar data under rainy and snowy conditions," *IEEE Intelligent Transportation Systems Magazine*, vol. 13, no. 1, pp. 197–209, 2020.
- [23] J. Wu, H. Xu, and J. Zhao, "Automatic lane identification using the roadside lidar sensors," *IEEE Intelligent Transportation Systems Magazine*, vol. 12, no. 1, pp. 25–34, 2018.
- [24] J. Wu, H. Xu, Y. Tian, Y. Zhang, J. Zhao, and B. Lv, "An automatic lane identification method for the roadside light detection and ranging sensor," *Journal of Intelligent Transportation Systems*, vol. 24, no. 5, pp. 467–479, 2020.
- [25] K. He, X. Zhang, S. Ren, and J. Sun, "Spatial pyramid pooling in deep convolutional networks for visual recognition," *IEEE transactions on pattern analysis and machine intelligence*, vol. 37, no. 9, pp. 1904–1916, 2015.
- [26] A. Bochkovskiy, C.-Y. Wang, and H.-Y. M. Liao, "Yolov4: Optimal speed and accuracy of object detection," *arXiv preprint arXiv:2004.10934*, 2020.
- [27] F. Chabot, M. Chaouch, J. Rabarisoa, C. Teuliere, and T. Chateau, "Deep manta: A coarse-to-fine many-task network for joint 2d and 3d vehicle analysis from monocular image," in *Proceedings of the IEEE conference on computer vision and pattern recognition*, 2017, pp. 2040–2049.
- [28] C.-T. Lin, S.-W. Huang, Y.-Y. Wu, and S.-H. Lai, "Gan-based day-to-night image style transfer for nighttime vehicle detection," *IEEE Transactions on Intelligent Transportation Systems*, vol. 22, no. 2, pp. 951–963, 2020.
- [29] P.-Y. Chen, J.-W. Hsieh, M. Gochoo, C.-Y. Wang, and H.-Y. M. Liao, "Smaller object detection for real-time embedded traffic flow estimation using fish-eye cameras," in *2019 IEEE International Conference on Image Processing (ICIP)*. IEEE, 2019, pp. 2956–2960.
- [30] A. Asvadi, L. Garrote, C. Premebida, P. Peixoto, and U. J. Nunes, "Multimodal vehicle detection: fusing 3d-lidar and color camera data," *Pattern Recognition Letters*, vol. 115, pp. 20–29, 2018.

- [31] Y. Zeng, Y. Hu, S. Liu, J. Ye, Y. Han, X. Li, and N. Sun, "Rt3d: Real-time 3-d vehicle detection in lidar point cloud for autonomous driving," *IEEE Robotics and Automation Letters*, vol. 3, no. 4, pp. 3434–3440, 2018.
- [32] M. Simony, S. Milzy, K. Amende, and H.-M. Gross, "Complex-yolo: An euler-region-proposal for real-time 3d object detection on point clouds," in *Proceedings of the European Conference on Computer Vision (ECCV) Workshops*, 2018, pp. 0–0.
- [33] Q. Jin, G. Wu, K. Boriboonsomsin, and M. Barth, "Improving traffic operations using real-time optimal lane selection with connected vehicle technology," in *2014 IEEE Intelligent Vehicles Symposium Proceedings*. IEEE, 2014, pp. 70–75.
- [34] Z. Wang, G. Wu, and M. J. Barth, "Cooperative eco-driving at signalized intersections in a partially connected and automated vehicle environment," *IEEE Transactions on Intelligent Transportation Systems*, vol. 21, no. 5, pp. 2029–2038, 2019.
- [35] A. Geiger, P. Lenz, and R. Urtasun, "Are we ready for autonomous driving? the kitti vision benchmark suite," in *2012 IEEE Conference on Computer Vision and Pattern Recognition*, 2012, pp. 3354–3361.
- [36] J. Redmon, S. Divvala, R. Girshick, and A. Farhadi, "You only look once: Unified, real-time object detection," in *Proceedings of the IEEE Conference on Computer Vision and Pattern Recognition (CVPR)*, June 2016.
- [37] J. Redmon and A. Farhadi, "Yolo9000: Better, faster, stronger," in *Proceedings of the IEEE Conference on Computer Vision and Pattern Recognition (CVPR)*, July 2017.
- [38] C. Hunt, "Tcp/ip network administration, 3rd edition," *Oreilly & Associates Inc*, 2002.
- [39] JoeLennon and JoeLennon, *Introduction to JSON*. Beginning CouchDB, 2009.